



HAL
open science

Mid-infrared integrated wideband operational dual-polarization Fourier-transform spectrometer

Qiankun Liu, Joan Manel Ramírez, Vladyslav Vakarin, Xavier Le Roux, Carlos Alonso-Ramos, Jacopo Frigerio, Andrea Ballabio, Enrico Talamas Simola, David Bouville, Laurent Vivien, et al.

► To cite this version:

Qiankun Liu, Joan Manel Ramírez, Vladyslav Vakarin, Xavier Le Roux, Carlos Alonso-Ramos, et al.. Mid-infrared integrated wideband operational dual-polarization Fourier-transform spectrometer. Integrated Optics: Devices, Materials, and Technologies XXIII, Feb 2019, San Francisco, United States. pp.34, 10.1117/12.2510728 . hal-02362469v2

HAL Id: hal-02362469

<https://hal.science/hal-02362469v2>

Submitted on 26 Jun 2020

HAL is a multi-disciplinary open access archive for the deposit and dissemination of scientific research documents, whether they are published or not. The documents may come from teaching and research institutions in France or abroad, or from public or private research centers.

L'archive ouverte pluridisciplinaire **HAL**, est destinée au dépôt et à la diffusion de documents scientifiques de niveau recherche, publiés ou non, émanant des établissements d'enseignement et de recherche français ou étrangers, des laboratoires publics ou privés.

Mid-infrared integrated wideband operational dual-polarization Fourier-Transform spectrometer

Qiankun Liu^{*a}, Joan Manel Ramirez^a, Vladyslav Vakarin^a, Xavier Le Roux^a, Carlos Alonso-Ramos^a, Jacopo Frigerio^b, Andrea Ballabio^b, Enrico Talamas Simola^b, David Bouville^a, Laurent Vivien^a, Giovanni Isella^b, Delphine Marris-Morini^a

^aCentre de Nanosciences et de Nanotechnologies (C2N), Université Paris Sud, CNRS, Université Paris Saclay, 92160 Palaiseau, France; ^bL-NESS, Dipartimento di Fisica, Politecnico di Milano, Polo di Como, Via Anzani 42, 22100 Como, Italy

ABSTRACT

Due to the unique vibrational/rotational frequencies in the mid infrared (MIR) fingerprint region, which scans from 500 to 1500 cm^{-1} , molecules can be assuredly identified and quantified. Thus integrated on-chip mid infrared spectroscopic systems, with low power consumption and high performance, would show great value for numerous applications, such as medical diagnosis, astronomy, chemical and biological sensing or security. Different solutions can be envisioned as on-chip integrated spectrometers, such as Fourier-Transform spectrometers, echelle gratings, or arrayed waveguide gratings. Integrated spatial heterodyne Fourier-Transform spectrometer (SHFTS) shows relaxed fabrication tolerances while applying a phase and amplitude correction algorithm. Meanwhile, it provides high optical throughput and high spectral resolution compared with AWG or echelle gratings. However, up to now in the literature, most of the development of Fourier-Transform based spectrometer is based on silicon-on-insulator operating in the near infrared typically at 1.55 μm wavelength. Thereby the development of integrated Fourier-Transform spectrometer operating in the MIR covering the wide fingerprint region is highly desirable. In this work, we experimentally demonstrate the first polarization insensitive Fourier-Transform spectrometer operating in the mid infrared beyond 5 μm wavelength. The fabricated FTS which is based on the graded-index Ge-rich SiGe platform, contains 19 Mach-Zehnder interferometers with a linearly increasing path difference. A spectral resolution better than 15 cm^{-1} has been demonstrated within an unprecedented spectral range of 800 cm^{-1} (5 to 8.5 μm wavelength).

Keywords: Mid-infrared, SiGe, spectroscopy

1. INTRODUCTION

Benefiting from the unique absorption in the mid-infrared fingerprint region, molecules can be assuredly identified and quantified directly through their transmission spectra without any additional reference process. It is thus particularly interesting to investigate on-chip integrated mid-infrared spectroscopic systems providing low power consumption, high-performance and multi-detection. A great potential for many applications is foreseen, such as medical diagnosis, chemical and biological sensing, and environmental monitoring to name a few [1–3]. Different solutions can be envisioned as integrated spectrometers, such as Fourier-Transform spectrometers (FTS) [4,5], echelle gratings [6], or arrayed waveguide gratings (AWG) [7]. Integrated spatial heterodyne Fourier-Transform spectrometers (SHFTS) show relaxed fabrication tolerances while applying a phase and amplitude correction algorithm. Meanwhile, it provides high optical throughput and high spectral resolution compared with AWG or echelle gratings ..

Integrated SHFTS typically relies on an array of Mach-Zehnder interferometers (MZIs) with linearly increasing path lengths to implement the spatial heterodyne spectroscopy. The input signal is retrieved using a correction algorithm through either the spatial-dependent interferogram [4] or temperature-dependent interferogram [8] of the spectrometer. Up to now, most of the demonstration of integrated Fourier-Transform spectroscopy are based on the silicon-on-insulator platform which provides a mature technology for the near-infrared or short-wave infrared (SWIR) operation. From all the investigation in literature, state-of-the-art integrated SHFTS have shown narrowband operation mainly at 1.55 μm range [4,5,8,9] and SWIR wavelength range below 4 μm wavelength [10]. Moreover, the operation is limited to single polarization because of the polarization dependence of beam splitter performances. However, controlling the polarization

of collected light is challenging especially for specific applications such as space satellites or unmanned aerial vehicles [11]. Dual polarization spectrometer is thus highly desirable.

While the SOI platform is typically limited to near-infrared and SWIR wavelength ranges, alternative materials have been used to demonstrate integrated photonics circuits operating at longer wavelengths in order to cover the wide fingerprint region in the mid-infrared range. Recent achievements include III-V-based wavelength multiplexer [12], chalcogenide waveguides and micro-disk resonators [13,14], suspended silicon waveguide [15], AWG and supercontinuum generation on Ge-on-Si [16,17], and SiGe alloy [18–20]. Most recently, we demonstrated a Ge-rich graded-index SiGe platform exhibiting an ultra-wideband operation in the LWIR wavelength range [21–28]. The Ge-rich graded-index SiGe platform shows i) extended transparency demonstrated up to 8.5 μm , and potentially up to 15 μm ; ii) high versatility of optical engineering ; iii) high 3rd order nonlinearity.

In this paper, we present the experimental results of an integrated SHFTS implemented in the Ge-rich graded-index SiGe platform, operating in an unprecedented wideband wavelength range in the LWIR between 5 μm (2000 cm^{-1}) to 8.5 μm ($\sim 1170 \text{ cm}^{-1}$) wavelengths, and working both for transverse electric (TE) and transverse magnetic (TM) polarizations. The developed SHFTS shows an experimental resolution of 12 cm^{-1} (14.5 cm^{-1}) for TE(TM) polarization and a free spectral range of 132 cm^{-1} .

2. DESIGN AND FABRICATION

The SHFTS implementation is based on an 11- μm -thick $\text{Si}_{1-x}\text{Ge}_x$ graded layer where the Ge concentration is linearly increasing from 0 to 0.79 ($\text{Si}_{0.21}\text{Ge}_{0.79}$) along the growth direction. A 2- μm -thick constant layer $\text{Si}_{0.2}\text{Ge}_{0.8}$ is then deposited at the top of the graded layer. The waveguides are 4 μm wide and the etching depth is 4 μm , providing propagation losses of around 2.5 dB/cm from 5 to 8.5 μm wavelengths for both TE/TM polarizations [24]. Multimode interferometers (MMI) are used as beam splitter.

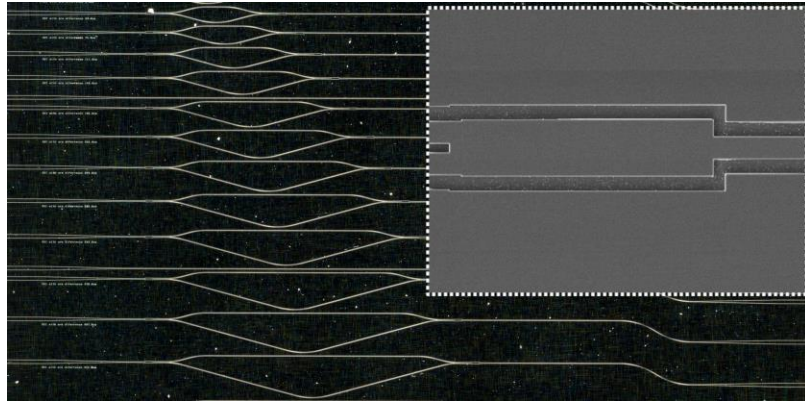


Figure 1. Optical microscope image of a part of the MIR spatial heterodyne Fourier-Transform spectrometer, (inset) SEM image of a multimode interferometer.

The integrated SHFTS is implemented as an array of 19 asymmetric MZIs in an area of 1.5 cm^2 using a multi-aperture configuration to provide high output throughput. Figure 1 shows the optical microscope image of the fabricated spectrometer and the scanning electron microscopy (SEM) image is shown in the inset of figure 1. The optical path difference (OPD) is introduced by each asymmetric Mach-Zehnder interferometer and is linearly increasing to a maximum path-length difference of ΔL_{max} . The device FSR and resolution ($\delta\nu$) can be determined by the maximum path difference and the number of MZIs (N) through the following equation with a unit of cm^{-1} :

$$\delta\nu = \frac{1}{\Delta L_{max} n_G} \quad (1)$$

$$FSR = \frac{\delta\nu N}{2} \quad (2)$$

where n_G is the group index, FSR represents the repetition property of the spectrometer while performing the signal retrieval process. A maximum path difference is set of $178.6 \mu\text{m}$ with a number of MZIs of 19, a theoretical resolution of 13.8 cm^{-1} and a FSR of 132 cm^{-1} can be thus obtained.

3. CHARACTERIZATION RESULTS

The fabricated SHFTS has been characterized through a free-space configuration using external cavity-based tunable quantum cascade lasers covering the $1170\text{-}2000 \text{ cm}^{-1}$ (5 to $8.5 \mu\text{m}$) spectral range. The laser operates in a pulsed regime of 100 kHz repetition rate, and a maximum mean power of 15 mW at 1540 cm^{-1} ($\sim 6.5 \mu\text{m}$) in TM polarization. A rotator is used at the output of the laser source to switch the polarization in TE while performing the measurement in TE polarization. The measurement is performed by butt-coupling in and out of each MZI by means of aspheric ZnSe lenses and on-chip adiabatic tapers. The transmission is then measured by an HgCdTe photodetector. The waveguide propagation losses and insertion loss for each MMI in the entire spectral range are compatible with previous works [24,25].

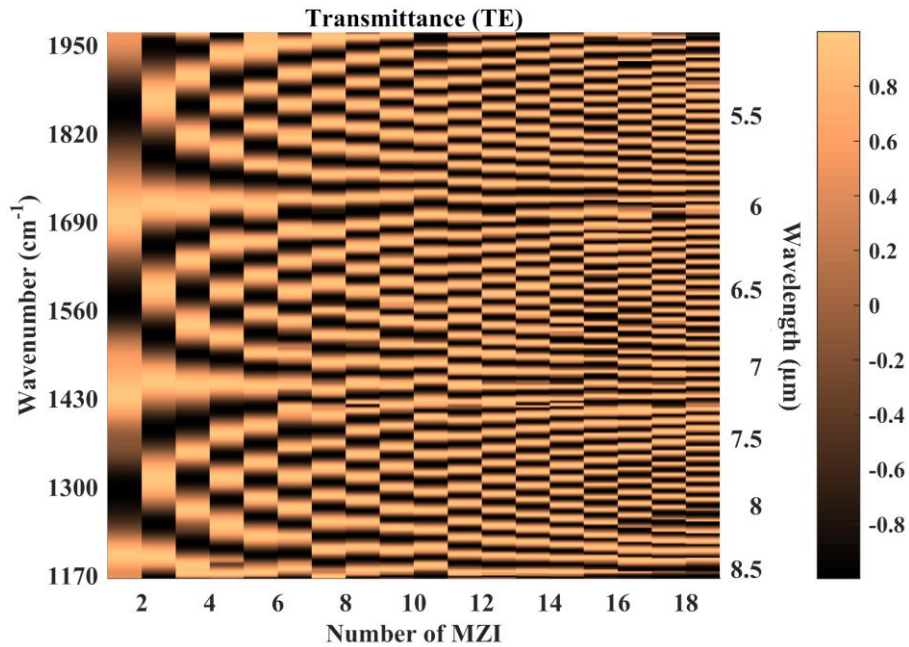


Figure 2. Experimental transmittance of each 19 MZIs for the fundamental transverse electric (TE) mode in the interferometer array of the spectrometer.

The operation principle of the SHFTS is the following : when an unknown input signal is sent at the SHFTS input, the transmission of each MZI is measured, forming the interference matrix. The input spectrum can then be reconstructed by means of Moore-Penrose algorithm through the multiplication of the interference matrix with the pseudo-inverse of the transformation matrix of the SHFTS. The Moore-Penrose algorithm provides effective correction of phase and amplitude errors arising from fabrication imperfections [4]. The transformation matrix is constructed in a preliminary stage, by recording the transmission spectrum of each MZI. A 3-step data processing is used to remove imperfections from the raw measurements, like the frequency dependence of the laser power: 1) normalization of MZI transmission by straight waveguide response; ii) subtraction of the mean value of the transmittance; iii) division by the envelope wavefunction.

The calibrated transformation matrix constructed for TE polarization is shown in figure 2. The Littrow frequency where all MZIs reach maximum transmission can be observed clearly for frequencies of 1185 , 1450 , and 1715 cm^{-1} , separated by two times the FSR of the device. This measurement gives a clear evidence of low phase distortion, proving the robustness of the Ge-rich SiGe waveguides to fabrication imperfections. The spectral retrieval for a monochromatic input is performed along the full operation range for both TE/TM polarizations, the retrieved spectra is shown in figure 3(a) and (c). The reported Ge-rich SiGe SHFTS allows spectral retrieval in a range of 800 cm^{-1} . It is worth to note that a

spectral range narrower than the device FSR has been considered for the retrieval process. A Gaussian function is applied in the spectral domain in order to reduce truncation ripple. The SHFTS resolution which is measured as the full width at half-maximum (FWHM) of the retrieved spectrum, are equal to 12 cm^{-1} (TE) and 14.5 cm^{-1} (TM) as shown in figure 3(b) and (d).

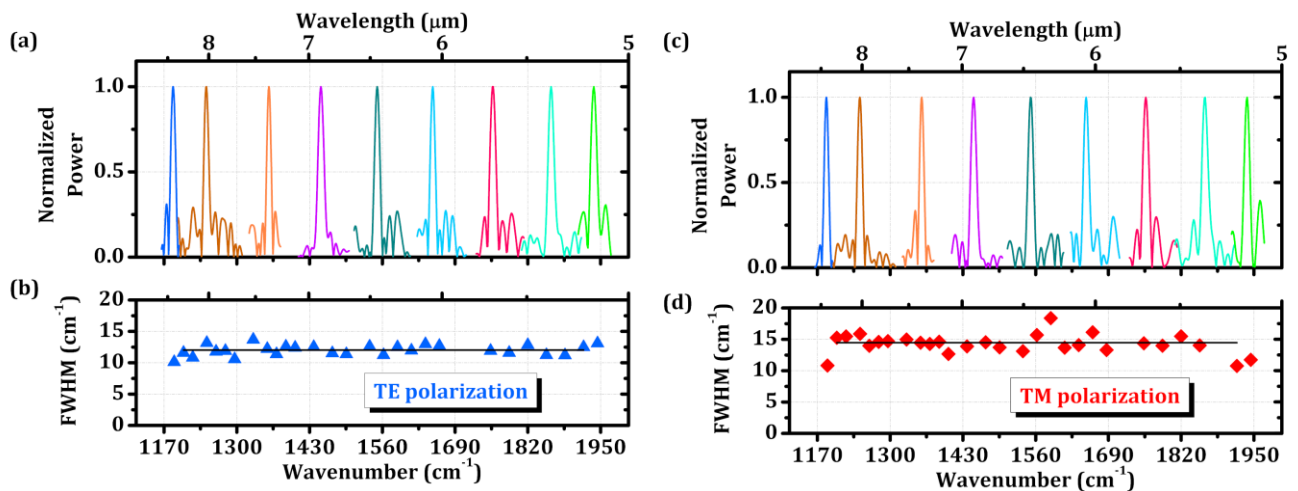


Figure 3. Experimentally retrieved spectra for a monochromatic input scanned between 1170 and 1950 cm^{-1} for TE (a) and TM (c) polarizations; measured FWHM of the retrieved signals in TE (b) and TM (d) polarizations, respectively.

Finally, a spectral retrieval has been repeated a few week later, using the same calibrated transformation matrix built in previous experiment, to evaluate the robustness of the fabricated device. Indeed, both the device resolution and possible temperature variation of the chip, which is not controlled in our setup, could affect the retrieved spectrum. Comparing the peak wavelength of retrieved spectrum with input wavelength, the error in frequency is always below 2 cm^{-1} in the entire experimental band.

4. CONCLUSION

In conclusion, we demonstrated a dual-polarization spatial heterodyne Fourier-Transform spectrometer based on Ge-rich graded-index SiGe waveguides. An unprecedented operational range of 800 cm^{-1} , with a FSR of 132 cm^{-1} has been reported. The experimental resolution is below 15 cm^{-1} for both TE/TM polarizations in the considered wavelength range from $5\text{ }\mu\text{m}$ (2000 cm^{-1}) to $8.5\text{ }\mu\text{m}$ ($\sim 1170\text{ cm}^{-1}$). The observation of Littrow wavelength shows a good robustness of the device design and fabrication against fluctuations of the waveguide effective index and optical path. This first demonstration of on-chip mid-IR FTS paves the route for the future investigation of robust, cost-effective and high performance multi-detection spectroscopic systems in the LWIR.

REFERENCES

1. J. Depciuch, E. Kaznowska, I. Zawlik, R. Wojnarowska, M. Cholewa, P. Heraud, and J. Cebulski, "Application of Raman Spectroscopy and Infrared Spectroscopy in the Identification of Breast Cancer," *Appl. Spectrosc.* **70**(2), 251–263 (2016).
2. H. Lin, Z. Luo, T. Gu, L. C. Kimerling, K. Wada, and A. Agarwal, "Review article Mid-infrared integrated photonics on silicon : a perspective," *7*(2), 393–420 (2018).
3. R. Soref, "Mid-infrared photonics in silicon and germanium," *Nat. Photonics* **4**(8), 495–497 (2010).
4. A. V. Velasco, P. Cheben, P. J. Bock, A. Del age, J. H. Schmid, J. Lapointe, S. Janz, M. L. Calvo, D.-X. Xu, M. Florjańczyk, and M. Vachon, "High-resolution Fourier-transform spectrometer chip with microphotonic silicon spiral waveguides," *Opt. Lett.* **38**(5), 706 (2013).
5. D. M. Kita, B. Miranda, D. Favela, D. Bono, J. Michon, H. Lin, T. Gu, and J. Hu, "High-performance and scalable on-chip digital Fourier transform spectroscopy," *Nat. Commun.* **9**(1), 1–7 (2018).
6. X. Ma, M. Li, and J. J. He, "CMOS-compatible integrated spectrometer based on echelle diffraction grating and

- MSM photodetector array," *IEEE Photonics J.* **5**(2), (2013).
7. A. Vasiliev, M. Muneeb, J. Allaert, J. Van Campenhout, R. Baets, and G. Roelkens, "Integrated Silicon-on-Insulator Spectrometer with Single Pixel Readout for Mid-Infrared Spectroscopy," *IEEE J. Sel. Top. Quantum Electron.* **24**(6), (2018).
 8. M. C. M. M. Souza, A. Grieco, N. C. Frateschi, and Y. Fainman, "Fourier transform spectrometer on silicon with thermo-optic non-linearity and dispersion correction," *Nat. Commun.* **9**(1), 1–8 (2018).
 9. M. Yang, M. Li, and J.-J. He, "Static FT imaging spectrometer based on a modified waveguide MZI array," *Opt. Lett.* **42**(14), 2675 (2017).
 10. M. Nedeljkovic, A. V. Velasco, A. Z. Khokhar, A. Delage, P. Cheben, and G. Z. Mashanovich, "Mid-Infrared Silicon-on-Insulator Fourier-Transform Spectrometer Chip," *IEEE Photonics Technol. Lett.* **28**(4), 528–531 (2016).
 11. D. F. V. James, "Change of polarization of light beams on propagation in free space," *J. Opt. Soc. Am. A* **11**(5), 1641–1643 (1994).
 12. C. Gilles, L. J. Orbe, G. Carpintero, G. Maisons, and M. Carras, "Mid-infrared wavelength multiplexer in InGaAs/InP waveguides using a Rowland circle grating," *Opt. Express* **23**(16), 20288 (2015).
 13. A. Gutierrez-Arroyo, E. Baudet, L. Bodiou, J. Lemaitre, I. Hardy, F. Faijan, B. Bureau, V. Nazabal, and J. Charrier, "Optical characterization at 77 μm of an integrated platform based on chalcogenide waveguides for sensing applications in the mid-infrared," *Opt. Express* **24**(20), 23109 (2016).
 14. H. Lin, L. Li, Y. Zou, S. Danto, J. D. Musgraves, K. Richardson, S. Kozacik, M. Murakowski, D. Prather, P. T. Lin, V. Singh, A. Agarwal, L. C. Kimerling, and J. Hu, "Demonstration of high-Q mid-infrared chalcogenide glass-on-silicon resonators," *Opt. Lett.* **38**(9), 1470 (2013).
 15. J. S. Penadés, A. Sánchez-Postigo, M. Nedeljkovic, A. Ortega-Moñux, J. G. Wangüemert-Pérez, Y. Xu, R. Halir, Z. Qu, A. Z. Khokhar, A. Osman, W. Cao, C. G. Littlejohns, P. Cheben, I. Molina-Fernández, and G. Z. Mashanovich, "Suspended silicon waveguides for long-wave infrared wavelengths," **43**(4), (2017).
 16. A. Malik, M. Muneeb, S. Pathak, Y. Shimura, J. Van Campenhout, R. Loo, and G. Roelkens, "Germanium-on-silicon mid-infrared arrayed waveguide grating multiplexers," *IEEE Photonics Technol. Lett.* **25**(18), 1805–1808 (2013).
 17. M. Yang, Y. Guo, J. Wang, Z. Han, K. Wada, L. C. Kimerling, A. M. Agarwal, J. Michel, G. Li, and L. Zhang, "Mid-IR supercontinuum generated in low-dispersion Ge-on-Si waveguides pumped by sub-ps pulses," *Opt. Express* **25**(14), 16116 (2017).
 18. M. Sinobad, C. Monat, B. Luther-davies, P. Ma, S. Madden, D. J. Moss, A. Mitchell, D. Allieux, R. Orobtcouk, S. Boutami, J.-M. Hartmann, J.-M. Fedeli, and C. Grillet, "Mid-infrared octave spanning supercontinuum generation to 85 μm in silicon-germanium waveguides," *Optica* **5**(4), 360 (2018).
 19. P. Barritault, M. Brun, P. Labeye, J.-M. Hartmann, F. Boulila, M. Carras, and S. Nicoletti, "Design, fabrication and characterization of an AWG at 45 μm ," *Opt. Express* **23**(20), 26168 (2015).
 20. M. Brun, P. Labeye, G. Grand, J.-M. Hartmann, F. Boulila, M. Carras, and S. Nicoletti, "Low loss SiGe graded index waveguides for mid-IR applications," *Opt. Express* **22**(1), 508 (2014).
 21. D. Marris-Morini, V. Vakarin, J. Manel Ramirez, Q. Liu, A. Ballabio, J. Frigerio, M. Montesinos, C. Alonso-Ramos, X. Le Roux, S. Serna, D. Benedikovic, D. Chrastina, L. Vivien, and G. Isella, "Germanium-based integrated photonics from near-to mid-infrared applications," *Nanophotonics* **7**(11), 1781–1793 (2018).
 22. J. M. R. Amirez, V. V. Akarin, J. F. Rigerio, P. C. Haisakul, C. Hrastina, X. L. E. R. Oux, A. B. Allabio, L. V. Ivien, G. I. Sella, and M. A. Orini, "Ge-rich graded-index Si 1- x Ge x waveguides with broadband tight mode confinement and flat anomalous dispersion for nonlinear mid- infrared photonics," **25**(6), 3020–3023 (2017).
 23. J. M. Ramírez, V. Vakarin, P. Chaisakul, J. Frigerio, C. Gilles, D. Chrastina, Q. Liu, G. Maisons, X. Le Roux, L. Vivien, M. Carras, G. Isella, and D. Marris-morini, "Ge-rich SiGe waveguides for mid-infrared photonics," **10108**, 2–7 (2017).
 24. J. M. Ramirez, Q. Liu, V. Vakarin, J. Frigerio, A. Ballabio, X. Le Roux, D. Bouville, L. Vivien, G. Isella, and D. Marris-Morini, "Graded SiGe waveguides with broadband low-loss propagation in the mid infrared," *Opt. Express* **26**(2), 870 (2018).
 25. V. Vakarin, J. M. Ramírez, J. Frigerio, A. Ballabio, X. Le Roux, Q. Liu, D. Bouville, L. Vivien, G. Isella, and D. Marris-Morini, "Ultra-wideband Ge-rich silicon germanium integrated Mach-Zehnder interferometer for mid-infrared spectroscopy," *Opt. Lett.* **42**(17), 3482 (2017).
 26. Q. Liu, J. M. Ramirez, V. Vakarin, X. Le Roux, C. Alonso-Ramos, J. Frigerio, A. Ballabio, E. Talamas Simola, D. Bouville, L. Vivien, G. Isella, and D. Marris-Morini, "Integrated broadband dual-polarization Ge-rich SiGe

mid-infrared Fourier-transform spectrometer," *Opt. Lett.* **43**(20), 5021 (2018).

Acknowledgment :

This project has received funding from the European Research Council (ERC) under the European Union's Horizon 2020 research and innovation programme (grant agreement N°639107-INSPIRE).